High-density electron–ion bunch formation and multi-GeV positron production via radiative trapping in extreme-intensity laser–plasma interactions

Remi Capdessus

CELIA, University of Bordeaux

Outline

- **Context**

- **Basic features**

- **Results**

  - overall interaction scenario

  - positron acceleration

  - ion mass influence

- **Conclusion**

Context

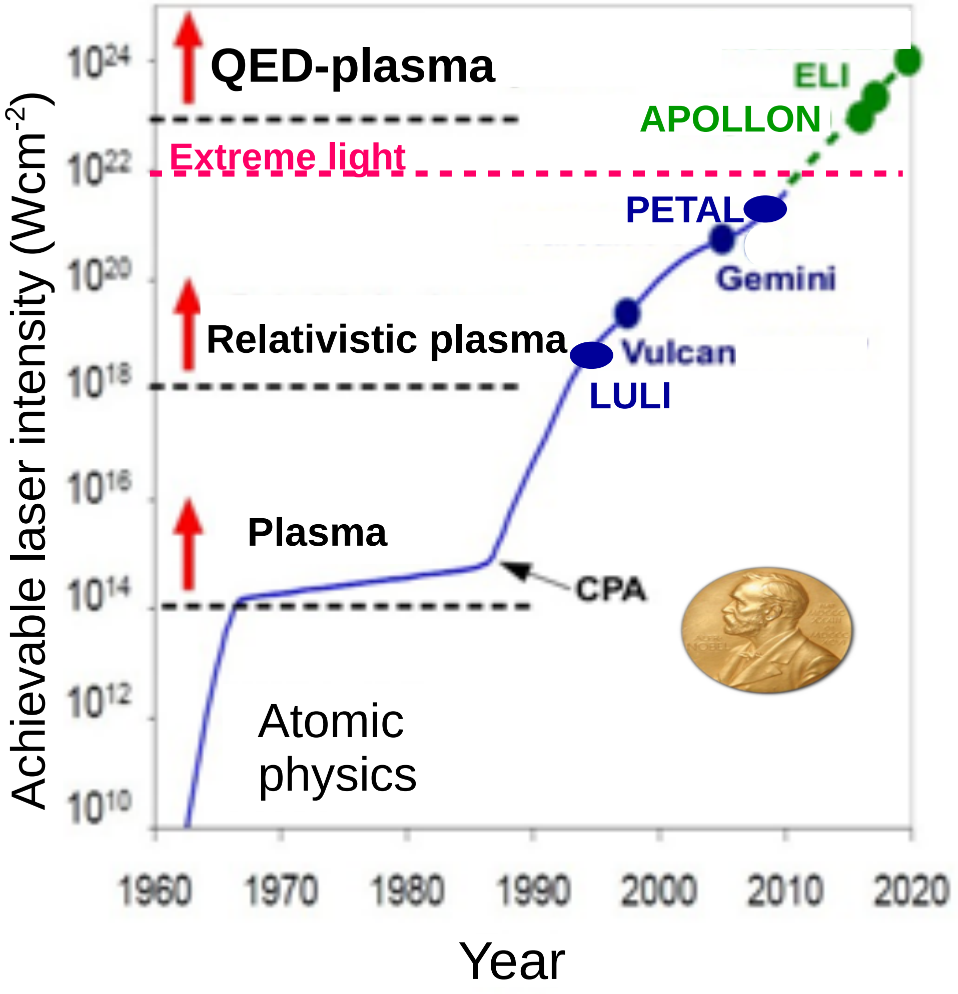

multi-PW laser facilities

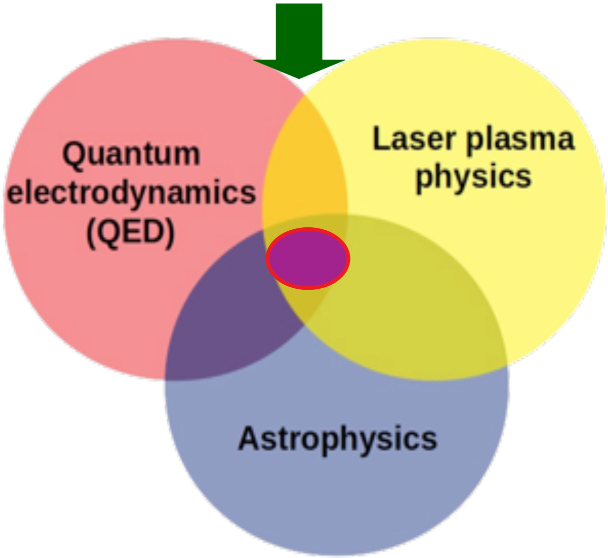

Context

- Advances in achievable laser intensity are enabling investigation of high-field QED processes, in particular in plasma environments where those processes couple with relativistic collective phenomena.

- High energy radiation + pair production → standards features of laser-matter interactions

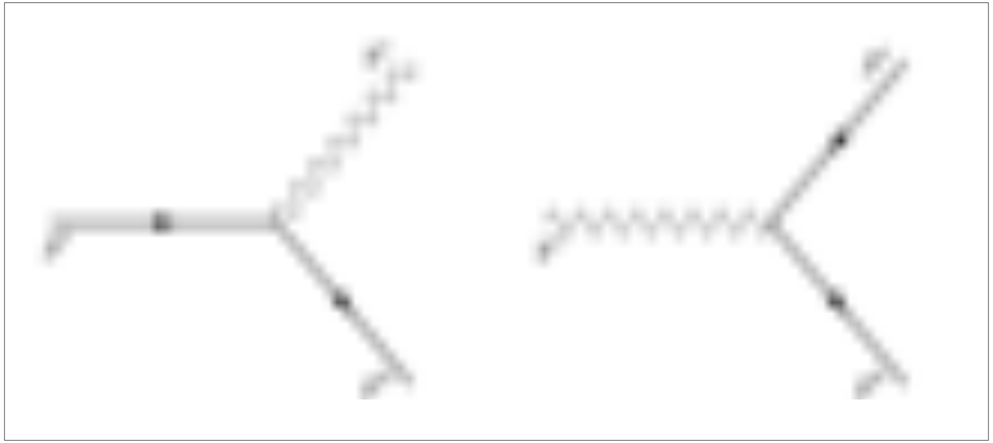

$$\chi_e = \left| \frac{F^{\mu\nu}}{E_s} \frac{p_{e\nu}}{m_e c} \right|$$

$$E_s = m_e c^3 / e\hbar \simeq 10^{16} \mathrm{V.cm}^{-1}$$

Sauter–Schwinger field

A. Di Piazza *et al*. Mod. Rev. Phys. **84** (2012).
P. Zhang *et al* . PoP **27**, 050601 (2020).

Context

- Advances in achievable laser intensity are enabling investigation of high-field QED processes, in particular in plasma environments where those processes couple with relativistic collective phenomena.

- High energy radiation + pair production → standards features of laser-matter interactions

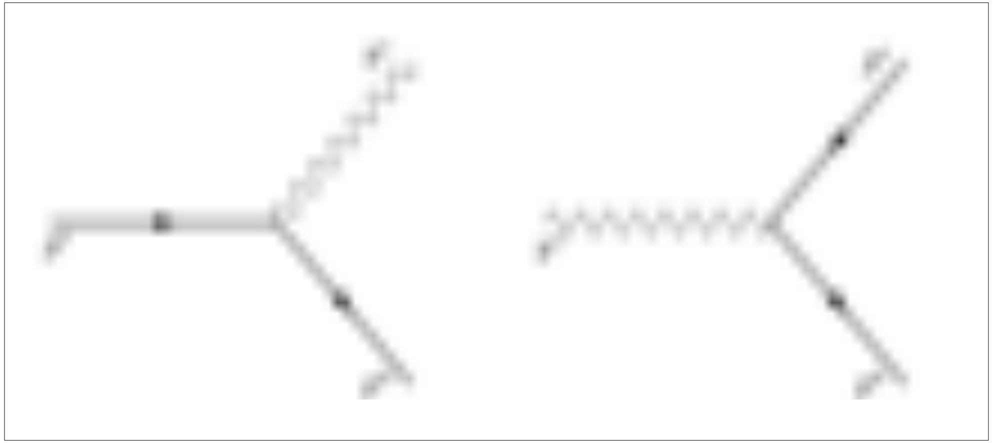

$$\chi_e = \left| \frac{F^{\mu\nu}}{E_s} \frac{p_{e\nu}}{m_e c} \right|$$

$$E_s = m_e c^3 / e\hbar \simeq 10^{16} \mathrm{V.cm}^{-1}$$

Sauter–Schwinger field

$$\chi_e = \boxed{\gamma_e \left(1 - \beta_{||}\right) a_0} \hbar\omega_L / m_e c^2$$

Plane wave

Doppler factor

A. Di Piazza *et al*. Mod. Rev. Phys. **84** (2012).
P. Zhang *et al* . PoP **27**, 050601 (2020).

Context

High field phenomenon: radiation backreaction (RR)

- The force that individual electrons in the plasma exert on themselves when they radiate
- Can dramatically alter electron dynamics

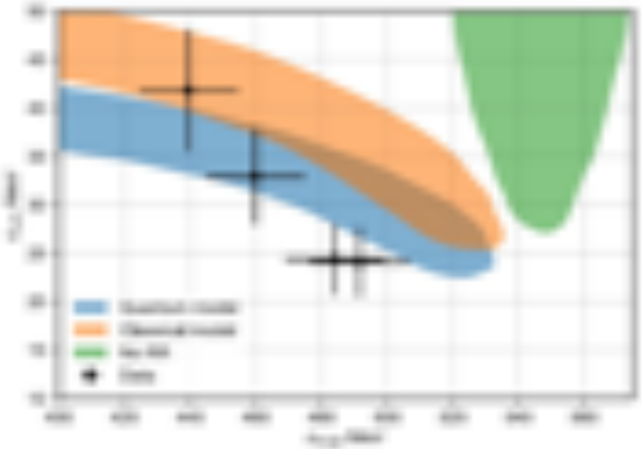

Cole *et al*. PRX **8** 011020 (2018)

→ recently evidenced experimentally in the collision of a laser-wakefield accelerated electron beam with an intense laser pulse at RAL, UK and within aligned crystals.

Other experimental evidences

Poder *et al*. PRX **8** 031004 (2018)

In crystals: Wistisen *et al*. Nat. Comm. **9** 795 (2018)

Theoretical & numerical work, see e.g.,

Landau and Lifshitz *The Classical Theory of Fields*

S.S. Bulanov *et al*. PRE **71** 016404 (2005)

Sokolov *et al*. PRE **81** 036412 (2010)

Schlegel and Tikhonchuk NJP **14** 073034 (2012)

Burton and Noble Contemp. Phys. **55** 2 (2014)

Basic features: particle-field

- The first fully relativistic treatment of radiation reaction was given by Dirac (1938).

$$m\ddot{x}^a = \underbrace{eF^a_b\dot{x}^b}_{\text{The Lorentz force}} + \underbrace{m\tau\left(\dddot{x}^a + \ddot{x}^b\ddot{x}_b\dot{x}^a\right)}_{\text{The self-force}}$$

c= 1

(+,-,-,-)
Used metric

- Suffers from well-known difficulties which render it unphysical such as runaway solutions, anti-causal solutions.
  (e.g. see D. A. Burton and A. Noble, Contemp. Phys. **55**, 110 (2014))

- To avoid unphysical solutions some theoretical model have been developed:

  - Landau and Lifshitz, *The classical theory of fields,* (1939).
  - Sokolov, JETP **109**, 207 (2009).
  - ...

Basic features: particle-field

The Landau-Lifshitz equation (~1939)

The RR force in LAD is a small correction to the Lorentz force of the applied fields.

$$\ddot{x}^a = -\frac{e}{m_e}\left(F^a_{\ b} + \tau \dot{x}^c \partial_c F^a_{\ b}\right)\dot{x}^b + \tau \frac{e^2}{m_e^2} \Delta^a_{\ b} F^b_{\ c} F^c_{\ d} \dot{x}^d$$

$$\Delta^a_{\ b} = \delta^a_b - \dot{x}^a \dot{x}_b$$

$$p^a = m\dot{x}^a$$

$$\tau = e^2/6\pi m_e$$

$$\dot{x}^2 = 1$$

Dominant term of the RR force (vectorial form)

$$\boldsymbol{F}_{RR} = -\frac{\mathcal{P}_{\text{cl.}}}{c^2}\boldsymbol{\beta}_e \qquad a_L \gg 1$$

$$\mathcal{P}_{\text{cl.}} = \frac{4\pi\alpha_f c}{3\lambda_c}\chi_e^2 m_e c^2 \qquad \gamma_e \gg 1$$

Basic features: particle-field

Limit of the classical approach

$$\chi_e \ll 1 \qquad \boldsymbol{F}_{RR} = -\frac{\mathcal{P}_{\mathrm{cl.}}}{c^2}\boldsymbol{\beta}_e$$

$$\mathcal{P}_{\mathrm{cl.}} = \frac{4\pi\alpha_f c}{3\lambda_c}\chi_e^2 m_e c^2$$

$$\chi_e \gtrsim 0.1 \qquad \boxed{\mathcal{P}_\gamma = g\left(\chi_e\right) P_{\mathrm{cl.}}}$$

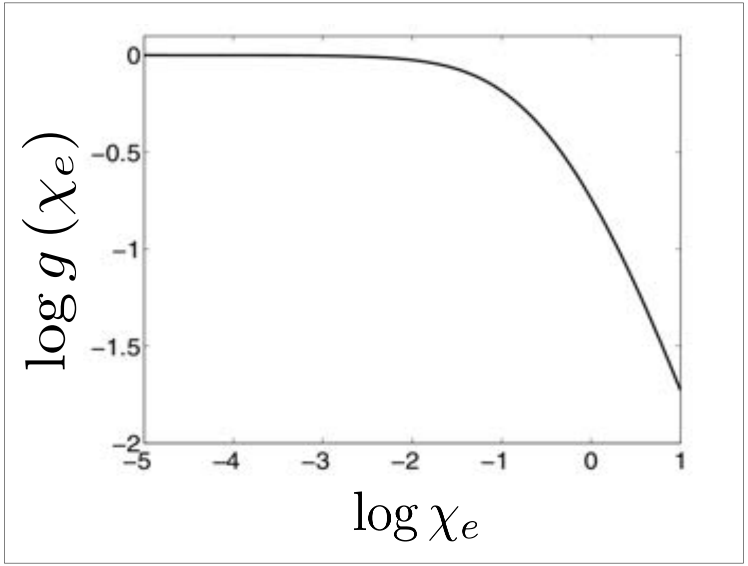

An electron cannot radiate a photon such that

$$\hbar\omega_\gamma \geq \left(\gamma_e - 1\right) m_e c^2$$

T. Erber, Rev. Mod. Phys. 38 626 (1966).
Sokolov and Ternov, *Synchrotron Radiation* (1968).

Basic features: laser-plasma interaction in extreme light

Interaction laser-plasma en Lumière extrême

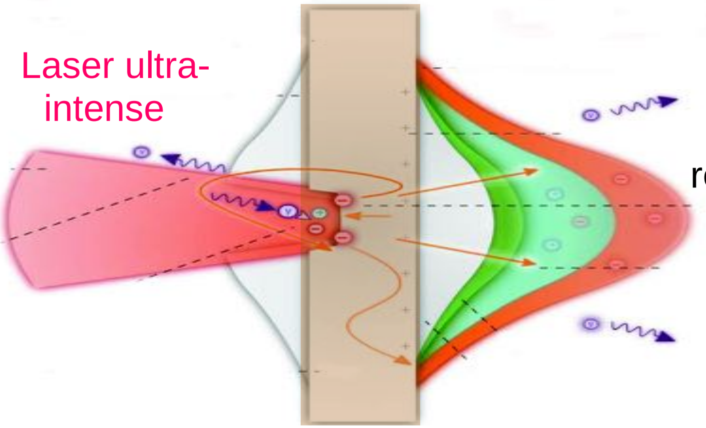

Relativistic laser-plasma interaction/UHI

+

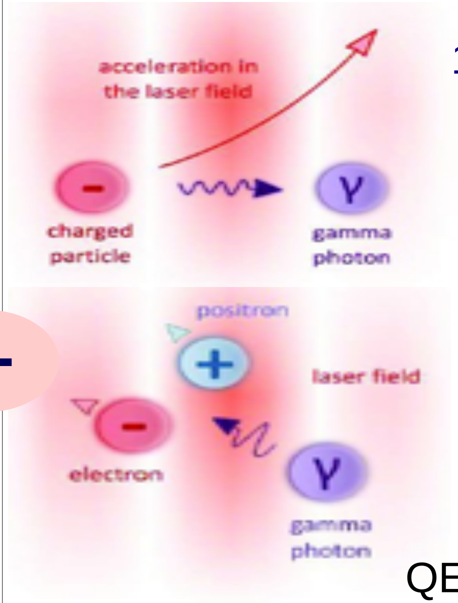

1. **gamma radiation + radiation reaction**

$$\dot{\mathbf{p}} = \mathbf{F}_{Le} - \frac{\mathcal{P}_\gamma}{c^2}\mathbf{v}_e$$

2. **Paire création**

QED processes

Basic features: laser-plasma interaction in extreme light

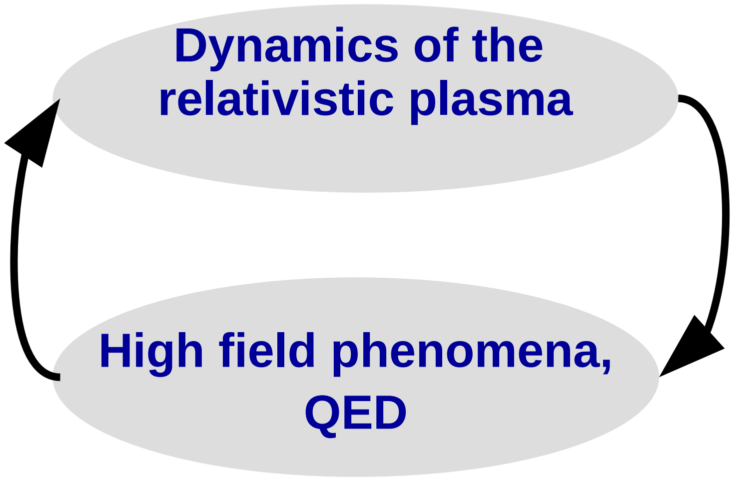

R. Capdessus *et al. PRL* (2013)

Basic features: laser-plasma interaction in extreme light

e.g. contraction of the electron
phase space volume

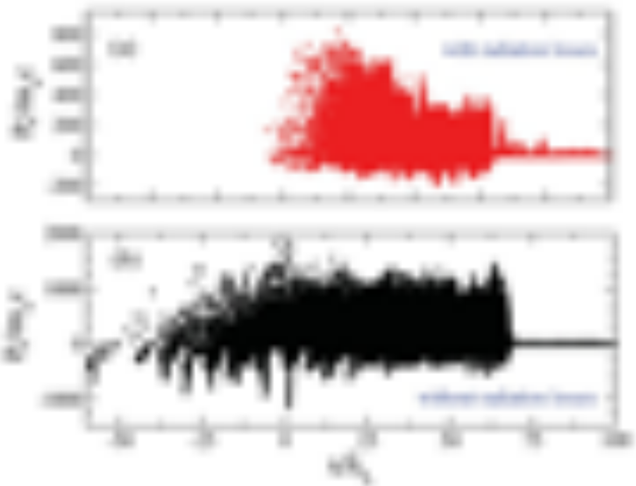

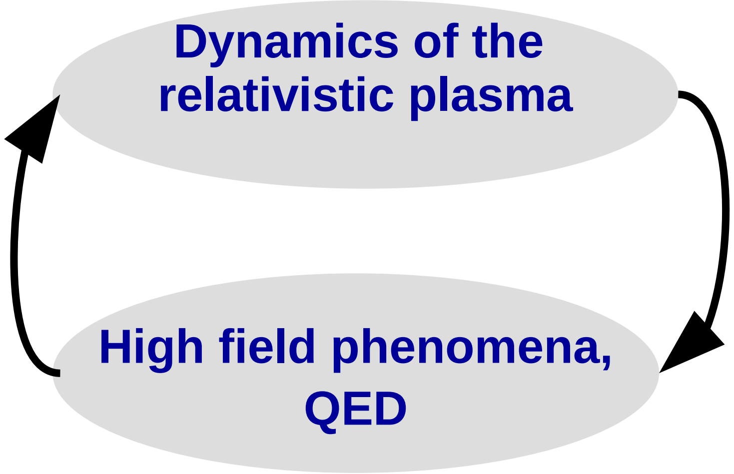

$$\frac{d\ln f_e}{dt} = -\boldsymbol{\nabla}_p.\mathbf{F}_{rr}$$

Tamburini *et al.* NIMPRA (2011)
R. Capdessus *et al.* PRE (2012)

Basic features: laser-plasma interaction in extreme light

e.g. contraction of the electron phase space volume

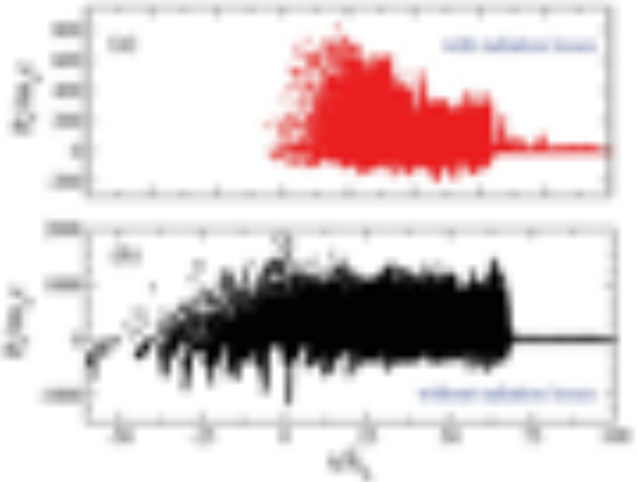

$$\frac{d \ln f_e}{dt} = -\boldsymbol{\nabla}_p . \mathbf{F}_{rr}$$

Tamburini *et al.* NIMPRA (2011)
R. Capdessus *et al.* PRE (2012)

Dynamics of the relativistic plasma

High field phenomena, QED

e.g. Ion mass influence on emitted radiation

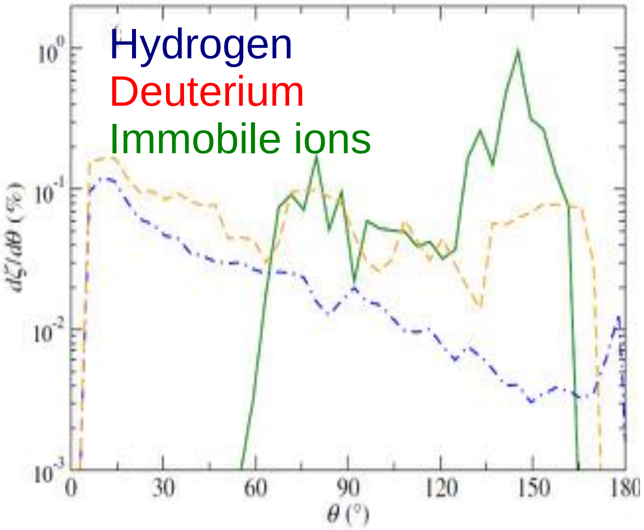

R. Capdessus *et al.* *PRL* (2013)

Results: purpose of the presented work

Generation, via radiative trapping, of highly compressed e–ion bunches inside the laser pulse, enabling copious production of gamma-ray photons and pairs.

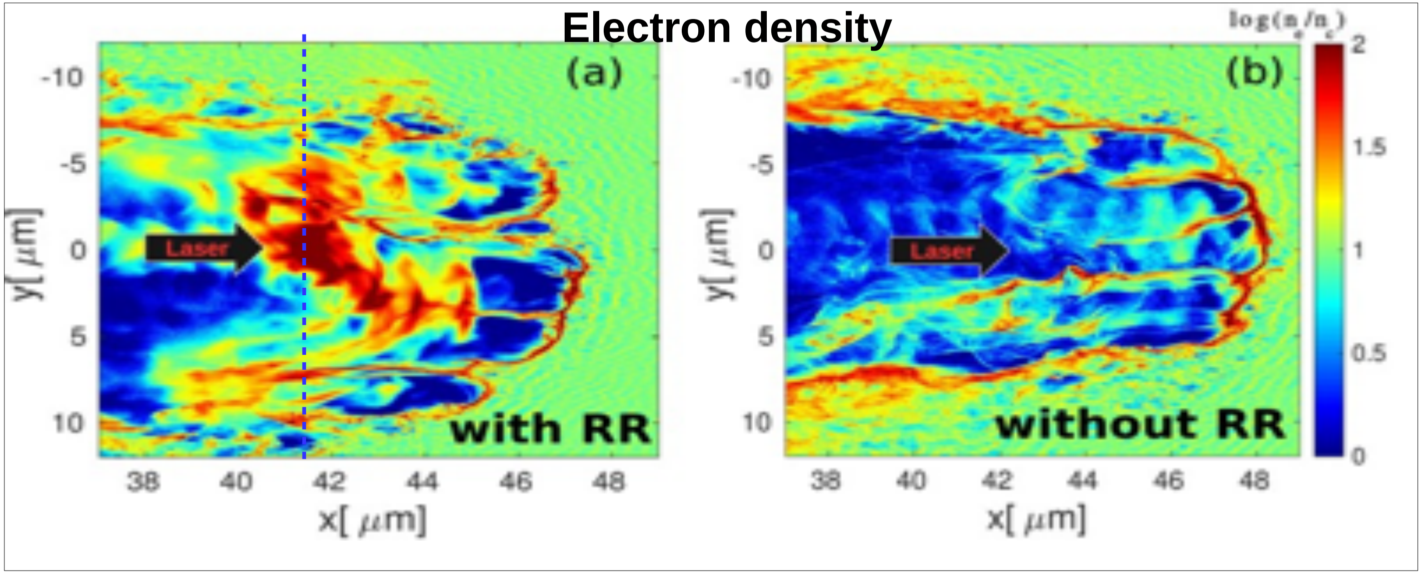

Balance between the ponderomotive force and the RR force → radiative trapping

Results

Simulation setup

- 2D3V PIC simulations performed with EPOCH[*].
- $I_L = 10^{24}\mathrm{W.cm}^{-2}$, circularly polarized
- $\tau_L = 30\ \mathrm{fs},\ \mathrm{spot}_{\mathrm{field}} = 5\mu m$ (Gaussian shape)
- Deuterium/hydrogen target with $n_0 = 10\ n_c$

$$\Rightarrow a_L \gg n_0/n_c \qquad a_L = E_L/m_e c\omega_L \simeq 850$$

[*] Arber *et al.* PPCF **57** 113001 (2015)

Results

Simulation setup

- 2D3V PIC simulations performed with EPOCH[*].
- $I_L = 10^{24} \mathrm{W.cm}^{-2}$, circularly polarized
- $\tau_L = 30\ \mathrm{fs},\ \mathrm{spot}_{\mathrm{field}} = 5\mu m$ (Gaussian shape)
- Deuterium/hydrogen target with $n_0 = 10\ n_c$

$$\Rightarrow a_L \gg n_0/n_c \qquad a_L = E_L/m_e c\omega_L \simeq 850$$

Framework of PIC code

Zhang et al. PoP **27**, 050601 (2020)

[*] Arber *et al.* PPCF **57** 113001 (2015)

Results

Simulation setup

- 2D3V PIC simulations performed with EPOCH[*].
- $I_L = 10^{24}\mathrm{W.cm}^{-2}$, circularly polarized
- $\tau_L = 30\ \mathrm{fs},\ \mathrm{spot}_{\mathrm{field}} = 5\mu m$ (Gaussian shape)
- Deuterium/hydrogen target with $n_0 = 10\ n_c$

$$\Rightarrow a_L \gg n_0/n_c \qquad a_L = E_L/m_e c\omega_L \simeq 850$$

Framework of PIC code

Zhang et al. PoP **27**, 050601 (2020)

[*] Arber *et al.* PPCF **57** 113001 (2015)

Results: the overall interaction scenario

Without RR

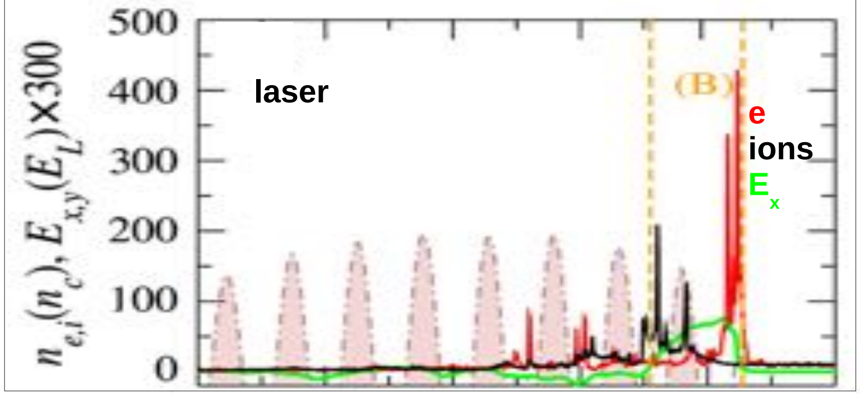

- The plasma electrons are pushed ahead in the laser's rising edge.
- When the electrostatic potential exceeds the ion kinetic energy most of the ions get reflected.
- A quasi-steady double-layer structure then arises at the front edge of the laser pulse **(B)**.

Shen and Zhang X NJP 20 053043 (2018).

Results: the overall interaction scenario

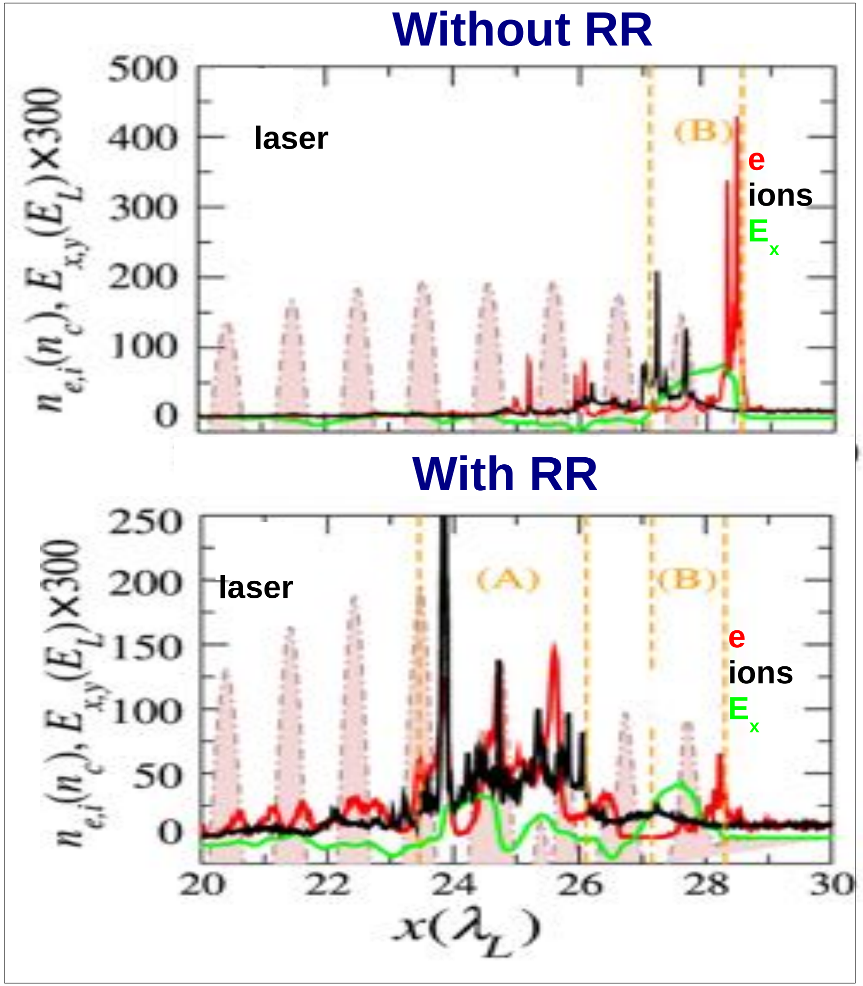

- The plasma electrons are pushed ahead in the laser's rising edge.
- When the electrostatic potential exceeds the ion kinetic energy most of the ions get reflected.
- A quasi-steady double-layer structure then arises at the front edge of the laser pulse (B).
- **When RR is enabled** the plasma wave excited at the laser edge is strongly altered.
- Rapid reflection of the returning electrons may not necessarily happen due to the straggling effect.
- → beginning of the bunch formation **(A)**

Bulanov *et al* 2004 PPR **30** 196 (2004)
Shen and Zhang X NJP **20** 053043 (2018).

Results: the overall interaction scenario

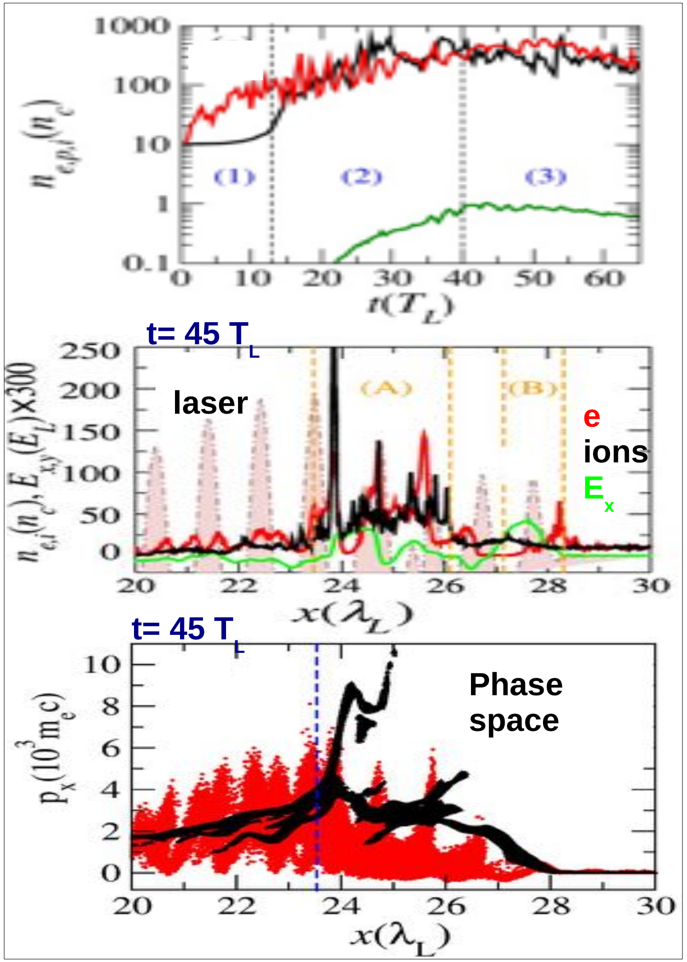

Main stages of the bunch formation

(1) The electron density near the laser peak starts increasing due to radiative cooling.

(2) The ions are then set into motion and compressed, thus restoring charge neutrality. Meanwhile, the production of electron–positron pairs kicks in.

(3) The quasineutral plasma bunch resulting from the compressed electrons and ions has reached a quasi-stationary maximum density and moves at an approximately constant velocity.

Results: the overall interaction scenario

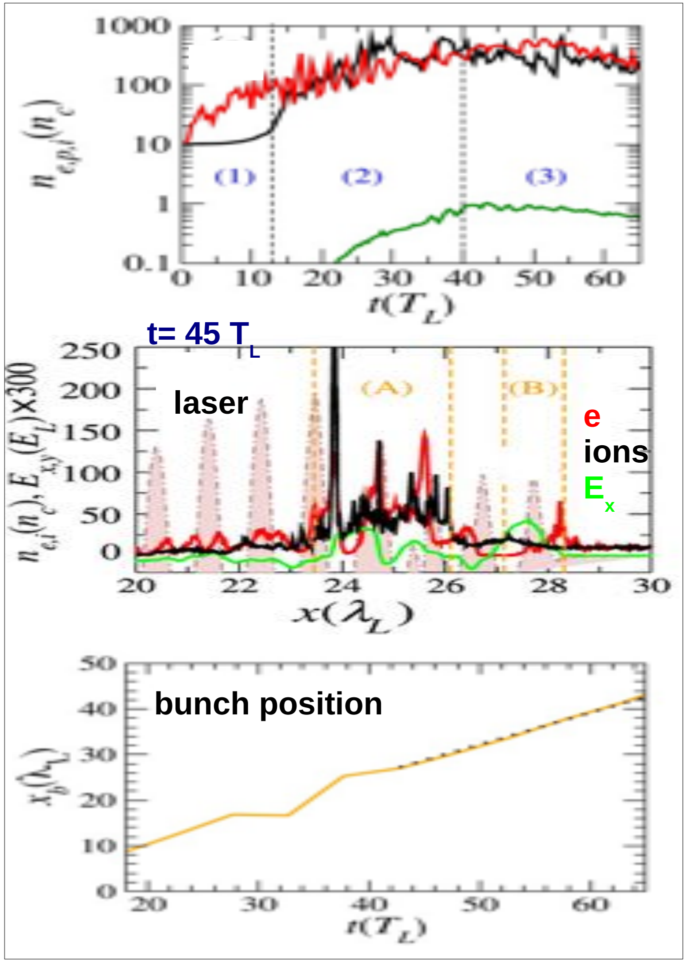

Main stages of the bunch formation

(1) The electron density near the laser peak starts increasing due to radiative cooling.

(2) The ions are then set into motion and compressed, thus restoring charge neutrality. Meanwhile, the production of electron–positron pairs kicks in.

(3) The quasineutral plasma bunch resulting from the compressed electrons and ions has reached a quasi-stationary maximum density and moves at an approximately constant velocity.

Results: the overall interaction scenario

Balance between the ponderomotive force and the RR force → radiative trapping

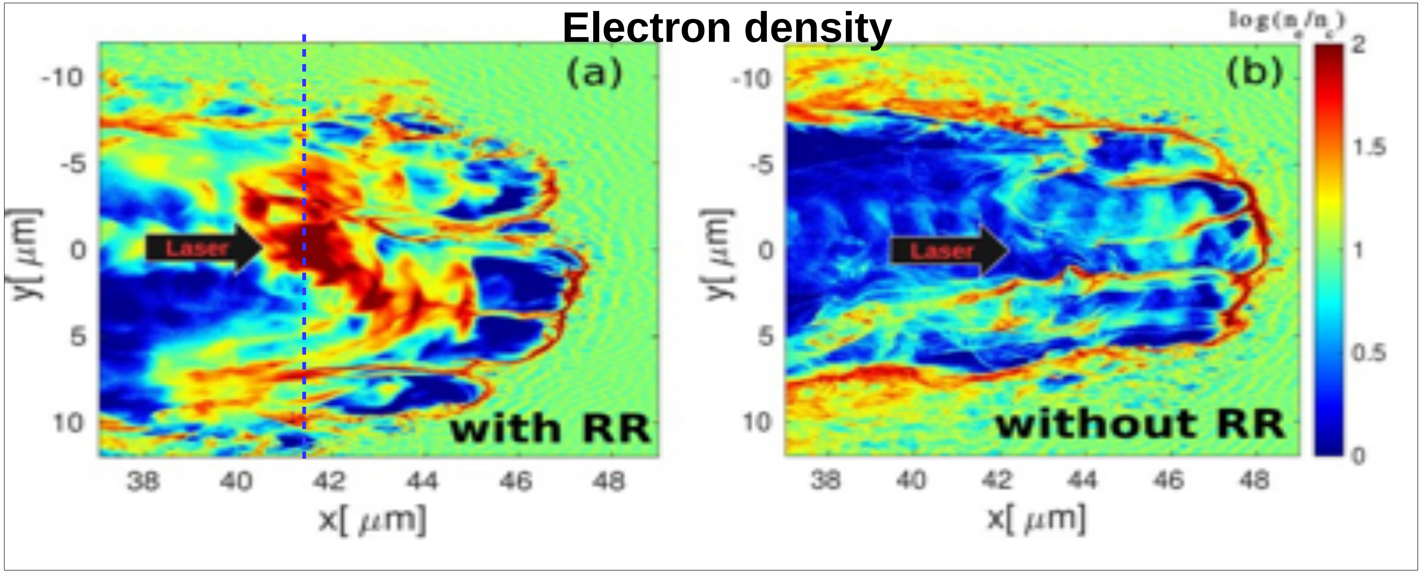

How to model such a structure ?

See also: L.L. Ji *et al*. PRL **112**, 145003 (2014) [first paper about RR trapping]

Results: analytical model

CP EM wave

rotating electric field

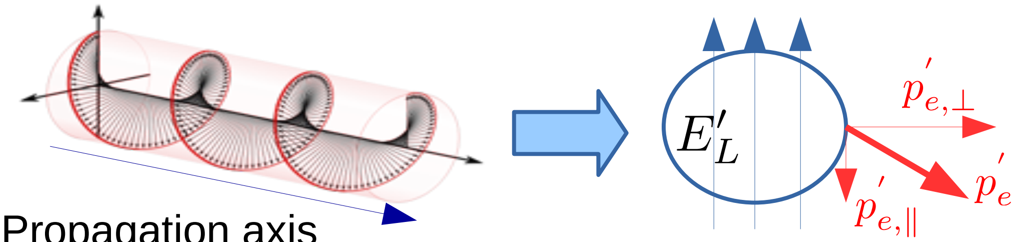

Propagation axis

$$E_L^{'} = E_L \frac{\Re\left(\Omega\right)}{\omega_L}$$

$$k_L' = B_L' = 0$$

Laboratory frame

EM wave frame

Akhiezer, Merenkov and Rekalo J. Phys. G: Nucl. Part. Phys. (1994)
Bashinov and Kim PoP **20** 113111 (2013)

Results: analytical model

Electromagnetic dispersion relation

CP EM wave

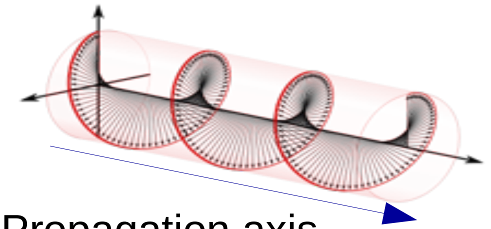

rotating electric field

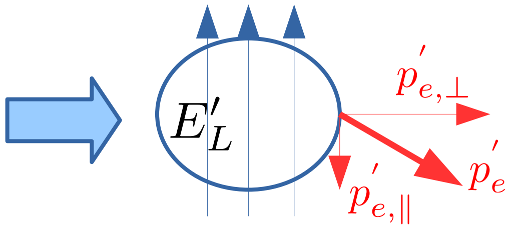

$$E'_L = E_L \frac{\Re(\Omega)}{\omega_L}$$

$$k'_L = B'_L = 0$$

Laboratory frame

EM wave frame

$$\omega^2 = k^2 c^2 + \Omega$$

$$\Omega^2 = \frac{\omega'^2_{pe}}{\gamma'_e (1 - i\mathcal{G})} + \frac{\omega'^2_{pi}}{\gamma'_i}$$

$$\mathcal{G} = \frac{\mathcal{P}_\gamma}{\gamma'_e m_e c^2 \Re(\Omega)}$$

$$\mathcal{P}_\gamma = \frac{4\pi\alpha_f c}{3\lambda_c} g(\chi_e) \chi_e^2 m_e c^2$$

Akhiezer, Merenkov and Rekalo J. Phys. G: Nucl. Part. Phys. (1994)
Bashinov and Kim PoP **20** 113111 (2013)

Results: analytical model

$$\chi_e = \frac{|F^{\mu\nu} p_{e\nu}|}{E_s} \simeq a_L \frac{p'_{e,\perp}}{m_e c} \frac{\hbar \Re\left(\Omega\right)}{m_e c^2} \simeq \sqrt{\frac{a_L}{g\left(\chi_e\right)\epsilon_{\mathrm{rad}}}} \frac{\left(1+\mathcal{X}^2\right)^{1/4}}{\sqrt{1+\mathcal{U}^2}} \frac{\hbar \omega_L}{\Gamma_b m_e c^2}$$

Results: analytical model

$$\chi_e = \frac{|F^{\mu\nu} p_{e\nu}|}{E_s} \simeq a_L \frac{p'_{e,\perp}}{m_e c} \frac{\hbar \Re(\Omega)}{m_e c^2} \simeq \sqrt{\frac{a_L}{g(\chi_e)\,\epsilon_{\mathrm{rad}}}} \frac{\left(1+\mathcal{X}^2\right)^{1/4}}{\sqrt{1+\mathcal{U}^2}} \frac{\hbar \omega_L}{\Gamma_b m_e c^2}$$

$$p'_{e,\perp} = \left(a_L g(\chi_e)\, \tau_r \Re(\Omega)\right)^{-1/2} + \mathcal{O}\left(a_L^{-1} \epsilon_{\mathrm{rad}}^{-1/3}\right)$$

$$\epsilon_{\mathrm{rad}} = \tau_r \Re(\Omega)$$

S.V. Bulanov *et al.* PRE **84**, 056605 (2011)

Results: analytical model

$$\chi_e = \frac{|F^{\mu\nu} p_{e\nu}|}{E_s} \simeq a_L \frac{p'_{e,\perp}}{m_e c} \frac{\hbar \Re(\Omega)}{m_e c^2} \simeq \sqrt{\frac{a_L}{g(\chi_e)\,\epsilon_{\mathrm{rad}}}} \frac{\left(1+\mathcal{X}^2\right)^{1/4}}{\sqrt{1+\mathcal{U}^2}} \frac{\hbar\omega_L}{\Gamma_b m_e c^2}$$

$$p'_{e,\perp} = \left(a_L g(\chi_e)\,\tau_r \Re(\Omega)\right)^{-1/2} + \mathcal{O}\left(a_L^{-1} \epsilon_{\mathrm{rad}}^{-1/3}\right)$$

$$\epsilon_{\mathrm{rad}} = \tau_r \Re(\Omega)$$

$$\Re(\Omega) = \frac{1+\mathcal{X}^2}{\sqrt{1+\mathcal{U}^2}} \sqrt{\Re(\Omega^2)}$$

$$\mathcal{U} \equiv \mathcal{X} / \left(1 + \sqrt{1+\mathcal{X}^2}\right)$$

$$\mathcal{X} \equiv \Im(\Omega^2) / \Re(\Omega^2)$$
$$= \mathcal{G} / \left[\alpha_i \left(1+\mathcal{G}^2\right) + 1\right]$$

S.V. Bulanov *et al.* PRE **84**, 056605 (2011)

Results: analytical model

$$\chi_e = \frac{|F^{\mu\nu} p_{e\nu}|}{E_s} \simeq a_L \frac{p'_{e,\perp}}{m_e c} \frac{\hbar \Re(\Omega)}{m_e c^2} \simeq \sqrt{\frac{a_L}{g(\chi_e)\,\epsilon_{\mathrm{rad}}}} \frac{\left(1+\mathcal{X}^2\right)^{1/4}}{\sqrt{1+\mathcal{U}^2}} \frac{\hbar\omega_L}{\Gamma_b m_e c^2}$$

$$\Rightarrow 2.3\chi_e^4 + 9.9\chi_e^3 - 2.7\chi_e^2 + \chi_e \simeq \frac{\chi_0}{\Gamma_b} \Rightarrow \chi_e \simeq 0.4 \qquad \chi_0 = \sqrt{\frac{a_L}{\omega_L \tau_r}} \frac{\hbar\omega_L}{m_e c^2}$$

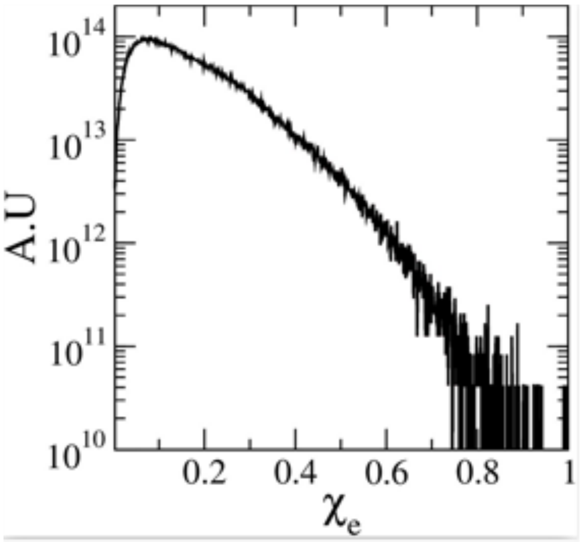

Bunch electrons χ_e (simulations)

Capdessus *et al.* NJP (2020)

Results: analytical model

Mean density of the bunch

$$\beta_b = \frac{\mathcal{B}}{1+\mathcal{B}} \quad \mathcal{B} = \sqrt{\frac{1+\mathcal{R}'}{(n_{i0}/n_c)\,(m_i/m_e)}}\frac{a_L}{2} \quad \mathcal{R}' = 0$$

Schlegel et al. PoP **16**, 083103 (2009).
Robinson *et al.* **51**, 024004 (2009).

Results: analytical model

Mean density of the bunch

$$\beta_b = \frac{\mathcal{B}}{1+\mathcal{B}} \quad \mathcal{B} = \sqrt{\frac{1+\mathcal{R}'}{(n_{i0}/n_c)\,(m_i/m_e)}}\frac{a_L}{2}$$ [bunch velocity] $\mathcal{R}' = 0$

$$\beta_g = \left(\frac{\partial\omega}{\partial\,\Re\,(k)}\right)_{\omega=\omega_L} \approx \sqrt{1-\frac{\Re\,(\Omega^2)}{\omega_L^2}}$$ [Laser group velocity]

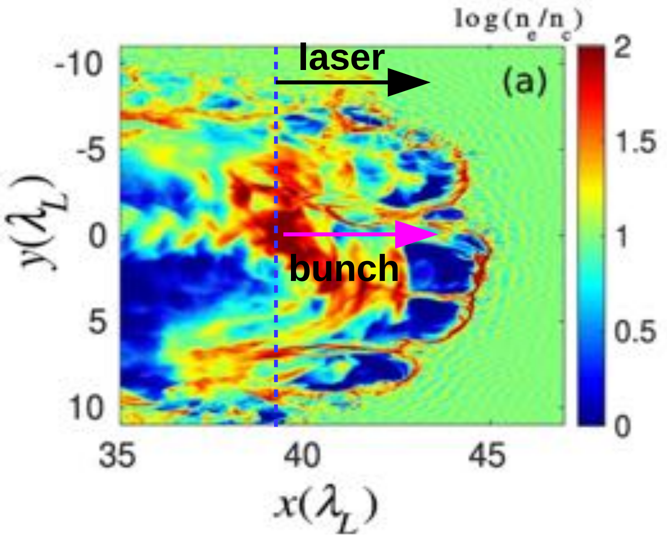

Brillouin *Wave Propagation and Group Velocity* (1960)
Loudon J. Phys. A: Gen. Phys. 3 233 (1970)
Gerasik V and Stastna M 2010 PRE 81 056602
Schlegel et al. PoP **16**, 083103 (2009).
Robinson *et al.* **51**, 024004 (2009).

Results: analytical model

Mean density of the bunch

$$\beta_b = \frac{\mathcal{B}}{1+\mathcal{B}} \quad \mathcal{B} = \sqrt{\frac{1+\mathcal{R}'}{(n_{i0}/n_c)\,(m_i/m_e)}}\frac{a_L}{2} \quad \mathcal{R}' = 0$$

$$\beta_g = \left(\frac{\partial\omega}{\partial\,\Re(k)}\right)_{\omega=\omega_L} \approx \sqrt{1-\frac{\Re\left(\Omega^2\right)}{\omega_L^2}}$$

$$\beta_b \approx \beta_g$$

$$\boxed{n_b = \frac{\mathcal{A}}{\left[\Gamma_b\left(1+\mathcal{A}\frac{Zm_e}{\gamma_i' m_i}\right)\right]} \simeq 500 n_c}$$

$$\mathcal{A} \equiv \gamma_e'\left(1+\mathcal{G}^2\right)$$

Simulation results

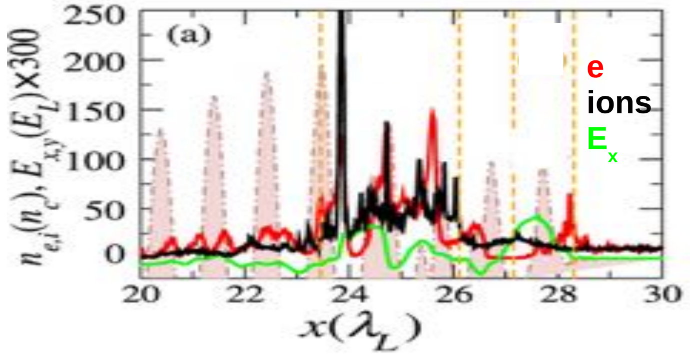

2 D results

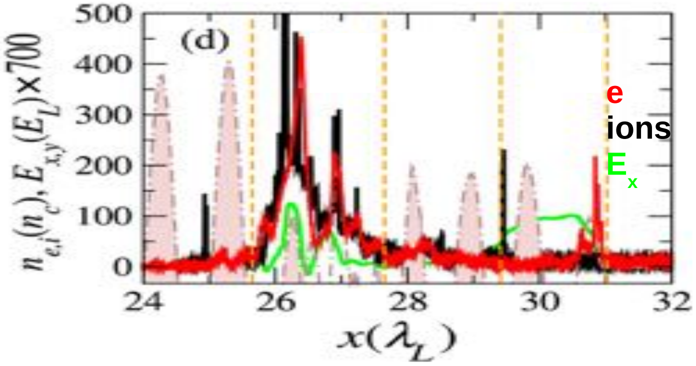

1 D results

Results: positron acceleration

- Creation of high energy photon via nonlinear Compton scattering $n\gamma_L + e \to e + \gamma$
- Creation of e^--e^+ pairs via the nonlinear Breit-Wheeler process $n\gamma_L + \gamma \to e^+ + e^-$

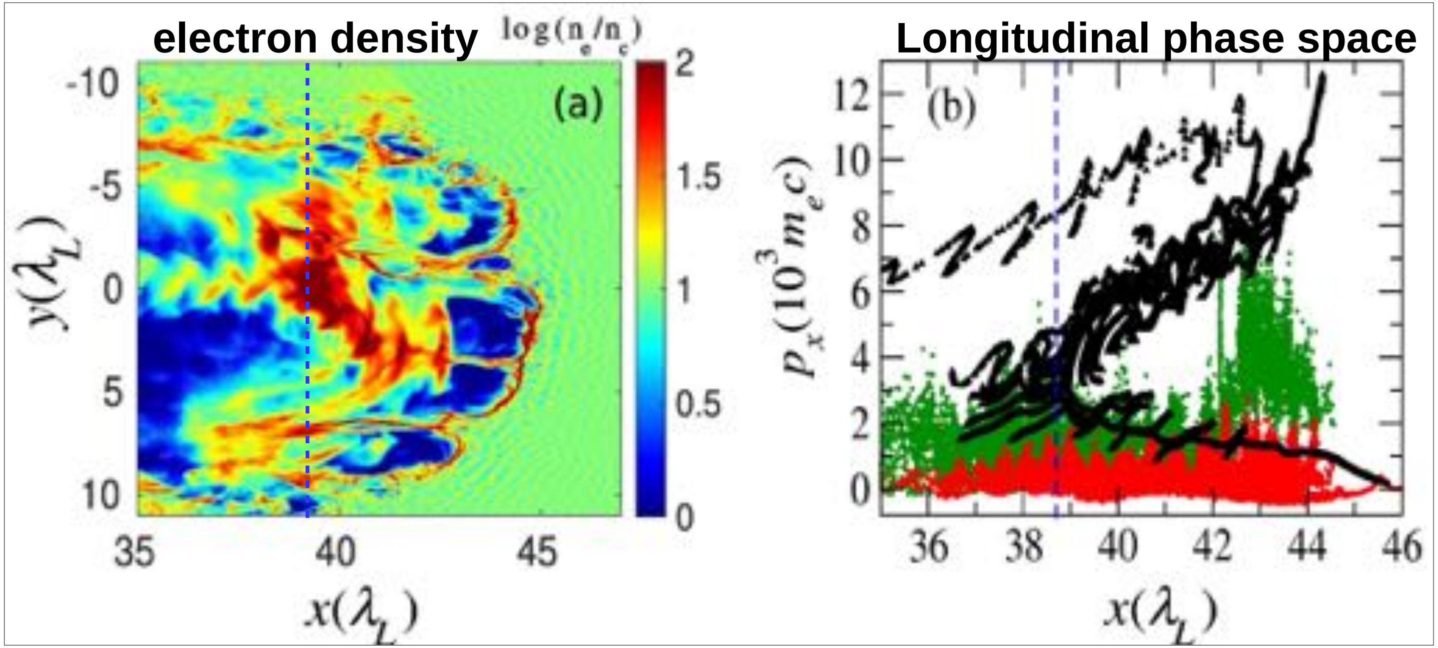

Deuterons

Electrons

Positrons

Results : positron acceleration

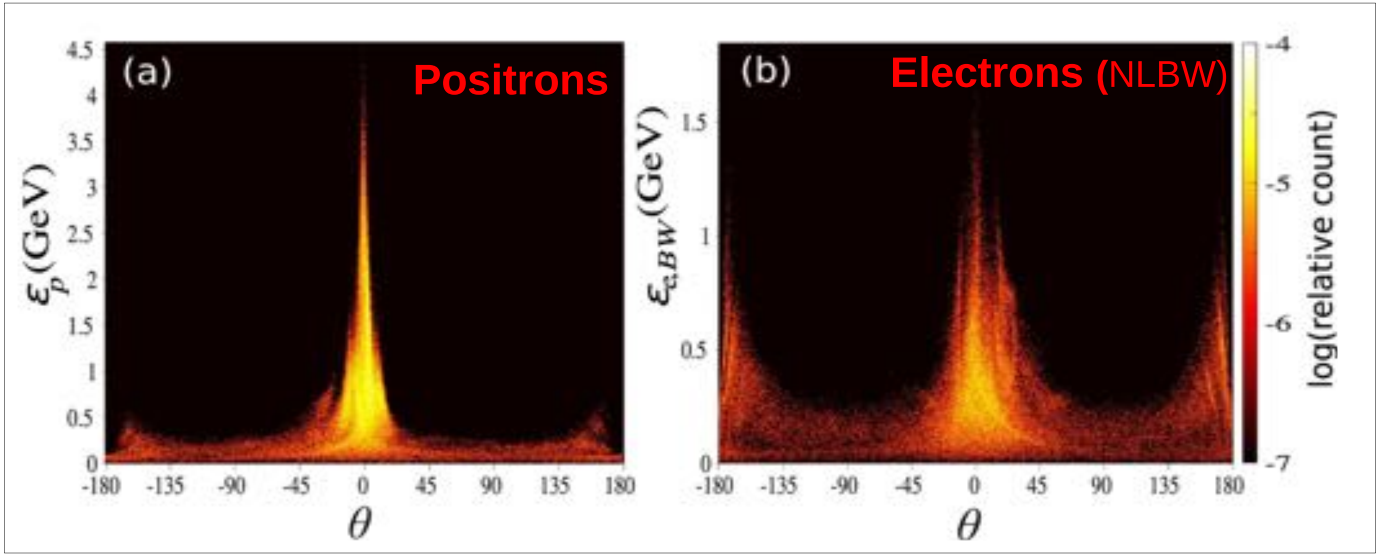

Capdessus *et al*. NJP (2020)

Results : positron acceleration

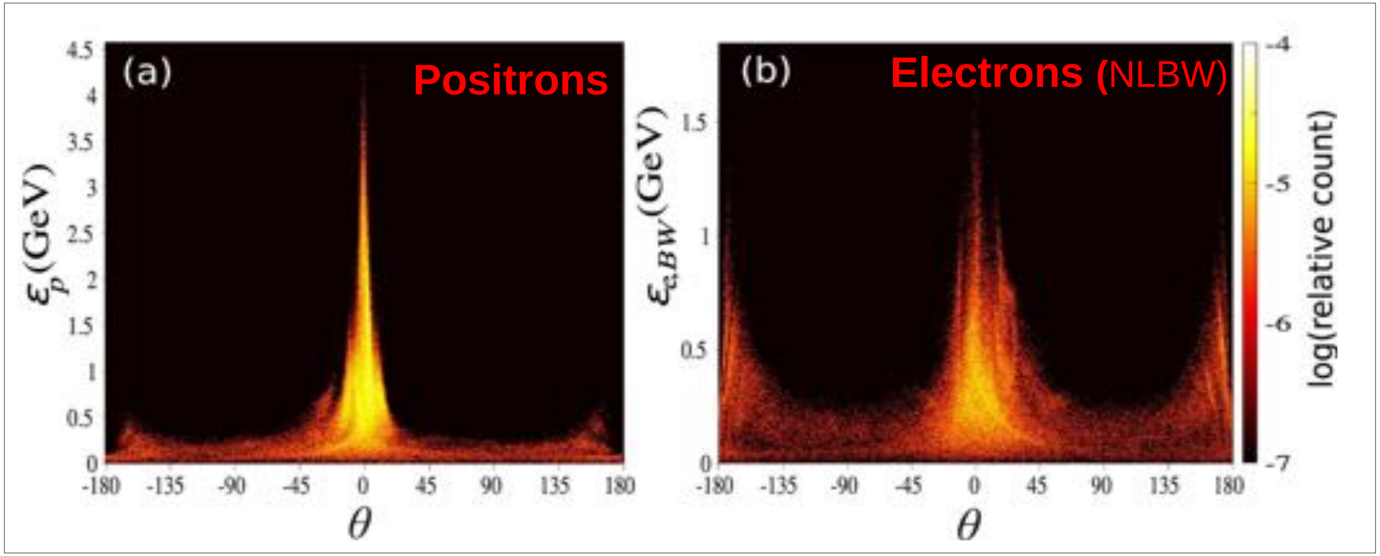

Why such differences of energies ?

Capdessus *et al*. NJP (2020)

Results : positron acceleration

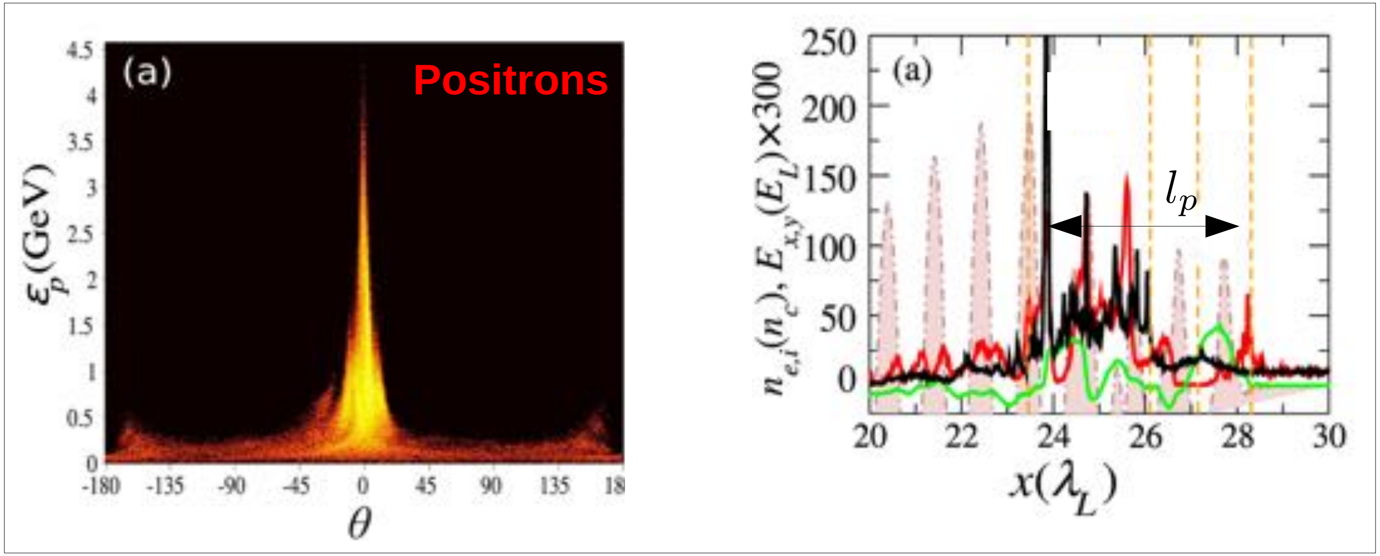

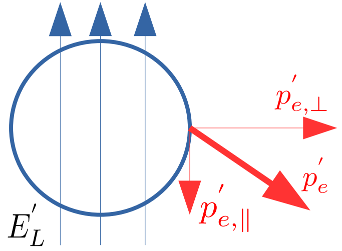

EM wave frame

$$\Delta\mathcal{E}_p \simeq \int_{l_p} dx\,(eE_x + F_{\mathrm{rad},x}) \simeq 2\pi\frac{l_p}{\lambda_L}m_e c^2\left(\bar{a}_L\frac{\beta_b\beta'_{p,\parallel}}{\Gamma_b} + a_x\right) \simeq 4\ \mathrm{GeV}$$

The radiation-modified Laplace force

Zel'dovich UFN **115** 161 (1975)
Fradkin PRL **42** 1209 (1979)

Capdessus *et al*. NJP (2020)

Results : Influence of the plasma ion mass

Laser energy Absorption

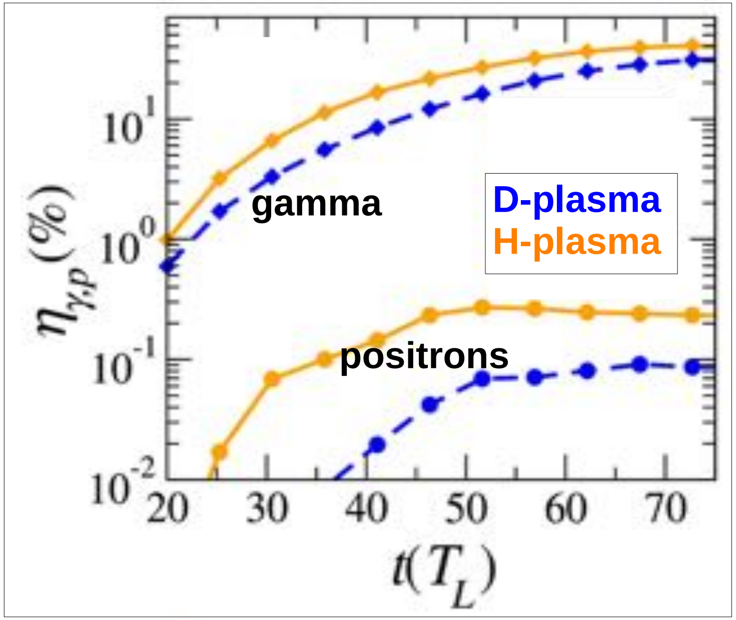

D-plasma → increases by ~ 2 the *positron absorption* compared with a **H-plasma**.

Results : Influence of the plasma ion mass

Laser energy Absorption

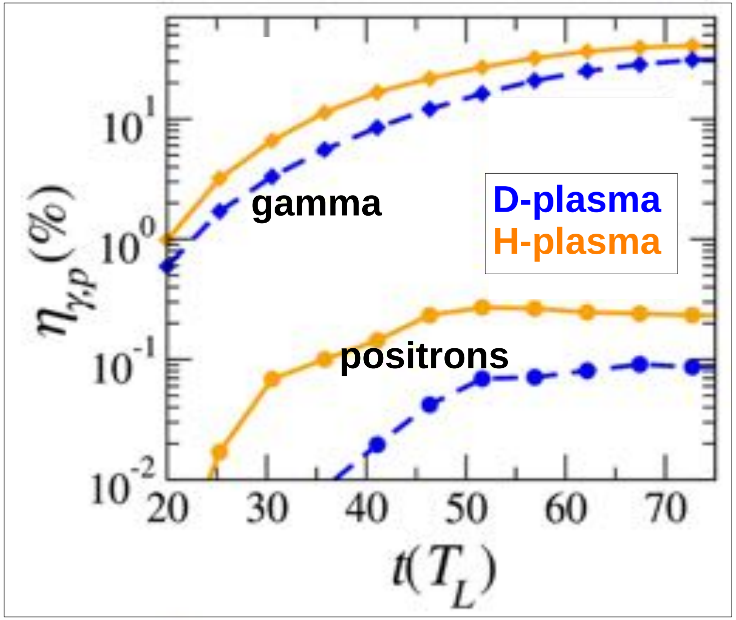

D-plasma → increases by ~ 2 the *positron absorption* compared with a **H-plasma**.

Energy spectra

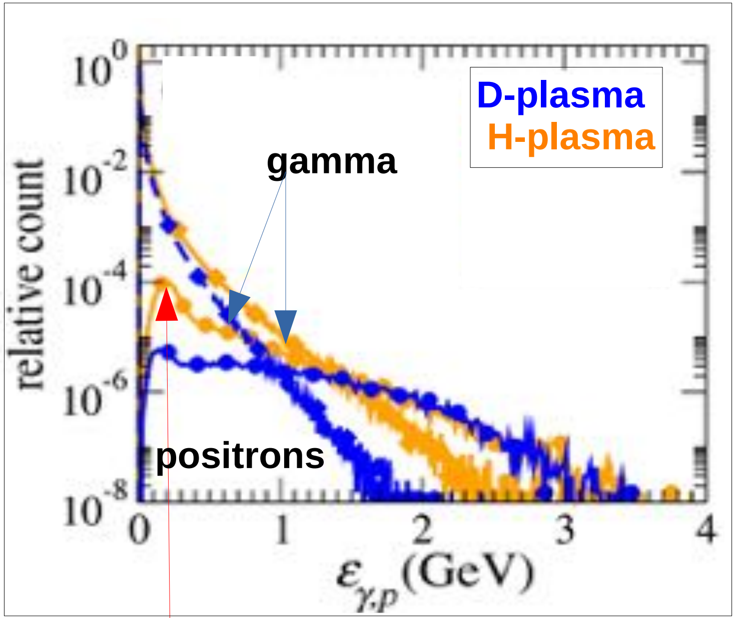

$$\langle\gamma_{\text{pos.}}\rangle \simeq \frac{\gamma'_e \Gamma_b a_L p'_{e,\perp} \hbar\omega_L}{2 m_e^2 c^3 \left(1+\Gamma_b^2 a_L \frac{p'_{e,\perp}}{m_e c}\frac{\hbar\omega_L}{m_e c^2}\right)} \simeq 400$$

Results : Influence of the plasma ion mass

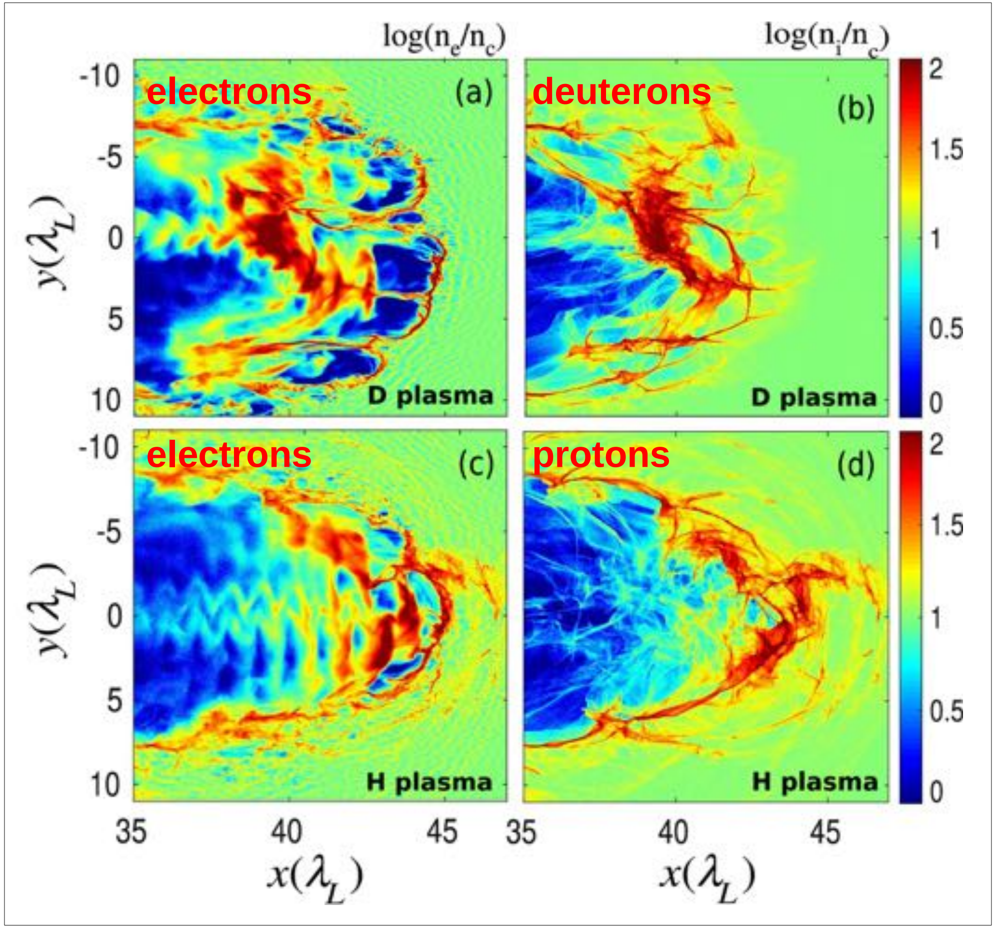

radiative trapping efficiency

The use of a H-plasma leads to a less stable and dense plasma bunch.

$$\epsilon_{\mathrm{rad}} = \Re\left(\Omega\right)\tau_r \simeq \Gamma_b^{-1}\omega_L\tau_r$$

→ increases with the ion mass

Capdessus *et al* NJP **22** 113003 (2020)

Conclusion

- Examination of how RR alters the interaction of a 10^{24} W.cm^{-2} laser pulse with a 10 n_c plasma.

- RR induces the formation of a piston-like, dense plasma bunch within the laser pulse.

- The positrons undergo efficient forward acceleration.

- Those results evidenced in a deuterium plasma, turn out to be sensitive to the ion mass.

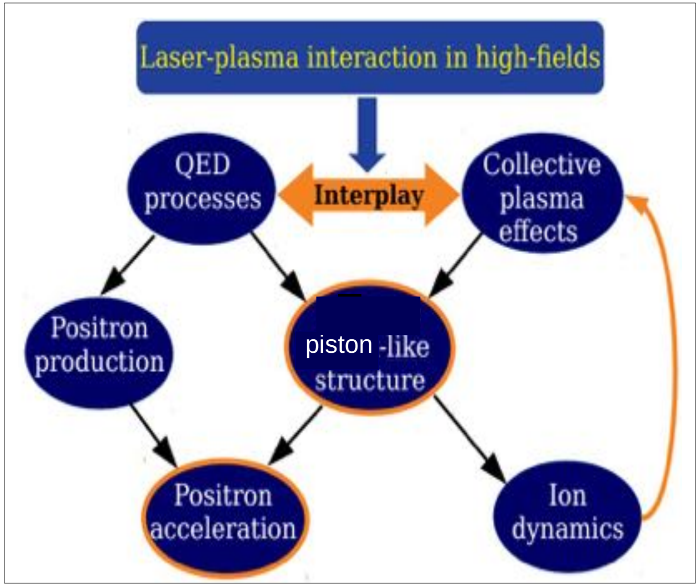

- The results could be useful for the design of high-field plasma experiments <u>especially</u> in view of producing dense pair plasma beams of relevance to laboratory astrophysics.

Thank you for your attention

see: R. Capdessus *et al* NJP **22** 113003 (2020)